# Robust Conceptual Design of Transonic Airfoils

Erik D. Olson*
*NASA Langley Research Center, Hampton, VA 23681*

**This paper describes an integrated, multi-fidelity analysis and heuristic design approach that can be used to derive initial airfoil designs for transonic flight. If successful, the final result is a geometry that can be expected to produce reasonable aerodynamic performance when used with higher order analysis methods. A key aspect of the methodology is the use of a "sonic-plateau" pressure distribution as the target distribution for inverse design. The sonic-plateau distribution is easily parameterized and has the advantage of automatically resulting in a smooth airfoil shape without any discontinuities built into the surface due to the presence of a shock in the target pressure distribution. Inverse design is performed on each airfoil using a parametrically defined pressure distribution at a reduced lift coefficient and Mach number from the design condition. The methodology is demonstrated by designing an airfoil at 38% of the wing semispan for a 737-200-like aircraft. The demonstration problem shows that the methodology is able to achieve rapid and robust convergence to the solution. The calculated drag-divergence Mach number for the designed airfoil was found to be sufficiently higher than the design Mach number, and the maximum thickness was close to the targeted value.**

## Nomenclature

| | |
|---|---|
| $\mathbf{b}$ | spanwise loading residual vector |
| $\boldsymbol{C}$ | twist influence matrix |
| $c$ | airfoil chord length |
| $c_d$ | sectional drag coefficient |
| $c_l$ | sectional lift coefficient |
| $c_m$ | sectional moment coefficient |
| $c_p$ | pressure coefficient |
| $i$ | index of spanwise loading reference station |
| $j$ | index of twist station |
| $M$ | Mach number |
| $n$ | load factor |
| $p$ | point |
| $S$ | wing reference area |
| $s$ | surface distance from stagnation, relative to chord |
| $t$ | airfoil thickness |
| $W$ | aircraft gross weight |
| $\mathbf{x}$ | twist change vector |
| $x$, $z$ | airfoil chordwise and normal coordinates |
| $\Lambda$ | sweep angle |

Sub/Superscripts

| | |
|---|---|
| $c/4$ | quarter-chord position |
| DD | drag divergence |
| design | design conditions |
| HSC | high-speed cruise |
| $l$ | lower surface |
| max | maximum |
| plat | sonic-plateau conditions |
| stag | stagnation point |

*Aerospace Engineer, Aeronautics Systems Analysis Branch, Senior Member AIAA.

| | |
|---|---|
| TE | trailing edge |
| $u$ | upper surface |
| $\infty$ | freestream conditions |
| $*$ | critical (sonic) value |

# I. Introduction

To accurately predict the mission performance of an aircraft concept, one must first obtain an accurate estimate of its aerodynamic characteristics. For designs that are similar to existing production aircraft, one can often use empirical relationships to arrive at a reasonably accurate estimate of the aerodynamic performance based on simple design variables, such as the wing planform shape, fuselage diameter, average wing section thickness, design Mach number, and design lift coefficient. Since these methods are based on a database of existing aircraft, they produce aerodynamic estimates which are representative of the lift and drag of the final production aircraft.

Newer design philosophies have increasingly included higher order analysis in the conceptual design stages to more directly model the physics of the flowfield and make the analysis more applicable to unconventional configurations. When higher order analysis methods are introduced in place of the previously used lower order methods, the complexity of the geometry modeling must be increased as well. The simple geometric models that were suitable for empirical relationships are now lacking crucial details about the model, such as the wing twist distribution and coordinates of the airfoils. The shape of the full outer moldline must be defined, but in doing so the geometry definition must represent a geometry that is well-designed. Otherwise, computational fluid dynamic analysis of these simple geometric models will produce aerodynamic polars which are unrepresentative of the as-built aircraft and will tend to exhibit problems with undesirable lift distributions and excessive drag.

This paper describes an integrated, multi-fidelity analysis and heuristic design approach that can be used to derive initial airfoil designs for transonic flight. If successful, the final result is a geometry that can be expected to produce reasonable aerodynamic performance when used with higher order analysis methods. The geometry can then serve as a starting point for a more detailed higher order design optimization to arrive at the final optimized configuration. To make the methodology suitable for the conceptual aircraft design phase, emphasis is placed on rapid and robust execution.

The next section, Section II, describes the methodology used to select the design flight conditions, define the spanwise lift distribution, and design the shape of airfoils along the span. Section III illustrates the use of the methodology by applying it to an example case. Finally, Section IV offers concluding remarks and recommendations for further research.

# II. Methodology

The envelope of potential cruise design conditions for a commercial subsonic transport aircraft is shown in Fig. 1. The maximum-range cruise Mach number is the nominal speed at which the aircraft cruises for its most efficient operation, whereas high-speed cruise is the speed at which the aircraft may fly to increase utilization without incurring an inordinately high penalty in efficiency. In addition to these speed variations, the lift coefficient can vary dramatically from its low value at the end of cruise when flying at the minimum cruise altitude, to the highest value near the maximum gross weight at the maximum top-of-climb altitude. For maximum fuel efficiency, the wing should be designed to have low drag anywhere within the cruise envelope; operating conditions outside of this envelope are associated with maneuvering and gusts, and so higher drag at these conditions will not impact the overall cruise efficiency [1].

The most challenging aerodynamic design condition is high-speed cruise at the maximum weight and altitude, where the wing is most likely to experience its highest drag due to shock formation. It therefore makes sense to use this point as the design condition for the wing. A wing designed for low drag at this design flight condition should have acceptable drag characteristics at lower speeds and/or lower weight and cruise altitude, where the transonic drag rise is alleviated.

This methodology follows a quasi-three-dimensional approach, where individual sections of the wing are created which produce the required lift coefficient at the design conditions while limiting the formation of shocks to avoid excessive drag. The full wing shape is then created by spanwise lofting between the designed sections. The individual steps in the design process are described in the following subsections.

### A. Spanwise Lift Distribution Design

To ensure that the spanwise distribution of aerodynamic load on the wing is representative of an efficient cruise condition, the twist distribution for the wing is first designed to produce an elliptical lift distribution at the nominal

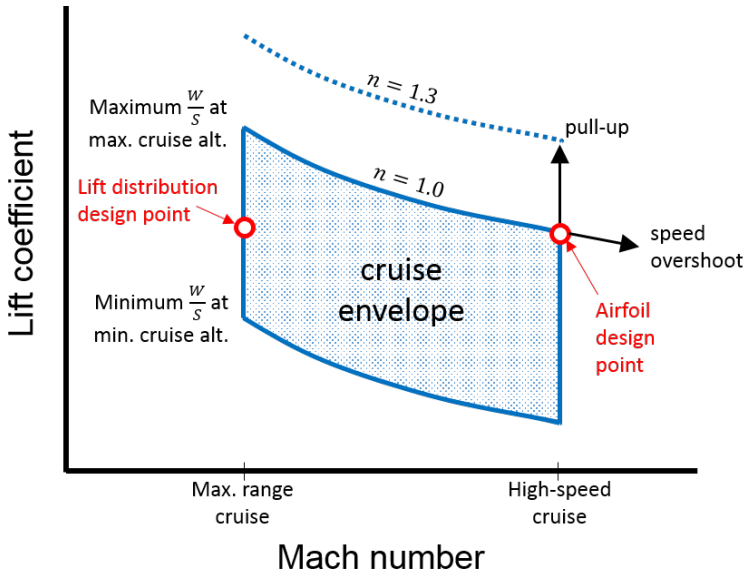


**Fig. 1 Cruise design space [1].**

maximum-range cruise condition (Fig. 1). The loading distribution is matched using a modal optimization process similar to that described in Ref. [2]. The desired twist distribution is found using a solution of the linear system $\boldsymbol{C}\mathbf{x} = \mathbf{b}$, where each element $C_{ij}$ is the change in spanwise loading coefficient at a spanwise reference station $i$ due to a change in twist at location $j$, and $b_i$ is the residual (the difference between the desired and actual loadings) at reference station $i$. Therefore, $x_j$ represents the change in twist at location $j$ required to match the target loading distribution.

To calculate the values of $C_{ij}$, the incidence at each airfoil station of the geometry model is individually perturbed by a small amount (e.g., one degree) and an analysis is performed to calculate the resulting residuals to produce column $j$ of matrix $\boldsymbol{C}$. Typically, there are more reference stations than twist locations, and the linear system is solved using a pseudo-inverse, or least-squares, solution. Aerodynamic analysis of the configuration is performed using ASWing, which uses a lifting-line aerodynamic analysis coupled with a non-linear equivalent-beam structural analysis [3]. Once the linear system has been solved, the $x$ vector is added to the existing twist distribution. The above process is iterated until satisfactory convergence is achieved.

### B. Airfoil Design Conditions

Once the twist distribution has been set to match the desired spanwise lift distribution at the maximum-range cruise conditions, the vehicle is analyzed again at high-speed cruise to determine the design conditions for each airfoil. At a given airfoil station, the lift coefficient at this flight condition, $c_{l_{\text{HSC}}}$, is extracted from the analysis results. In order to account for the effects of wing sweep, the design Mach number for each airfoil is equal to the freestream Mach number at high-speed cruise conditions, adjusted by the local quarter-chord sweep angle [1]:

$$M_{\text{design}} = (M_\infty)_{\text{HSC}} \cos\left(\Lambda_{c/4}\right) \tag{1}$$

Likewise, the design lift coefficient is

$$c_{l_{\text{design}}} = c_{l_{\text{HSC}}} / \cos^2\left(\Lambda_{c/4}\right) \tag{2}$$

To ensure that the vehicle is able to cruise at the high-speed condition without a significant drag penalty, it is necessary that drag divergence occurs at conditions outside the cruise envelope. The drag-divergence Mach number, $M_{\text{DD}}$, is defined as the Mach number at which

$$\frac{\partial c_d}{\partial M} = 0.10 \tag{3}$$

$M_{\text{DD}}$ is required to be greater than the design Mach number, e.g., $M_{\text{DD}} \geq 1.01 M_{\text{design}}$.

A number of methodologies exist in the literature for inverse design of transonic airfoils [4–10]. In general, these methodologies perform inverse design of the airfoil directly at the design flight condition, where shock discontinuities

tend to be present. When defining the target pressure distribution for the airfoil, the location and strength of the shock is not readily apparent and can be difficult to parameterize. In addition, performing inverse design using a target pressure distribution containing a shock can in turn result in a discontinuity in the airfoil surface which must be patched to restore the smooth surface for proper off-design performance.

A unique aspect of the methodology presented in this paper is the use of the "sonic-plateau" pressure distribution as the basis for inverse design of the airfoil. This distribution was used in the design of the original matrix of NASA supercritical airfoils [11]. At a particular combination of Mach number, $M_{\text{plat}}$, and lift coefficient, $c_{l_{\text{plat}}}$ (Fig. 2), the pressure coefficient on the surface rapidly decreases at the nose and reaches a value on the upper surface which is just above the critical pressure coefficient, $c_p^*$, corresponding to a velocity just below Mach 1. This pressure coefficient is maintained along the upper-surface plateau region before increasing steadily toward the trailing edge. To make up for the lift lost by restricting the upper-surface velocity to subsonic values, additional lift is carried by the higher pressure coefficients toward the trailing edge of the lower surface. Using this shock-free distribution allows for a simple parameterization of the shape of the distribution and avoids the discontinuities that can arise in the designed airfoil surface due to including a shock in the target distribution.

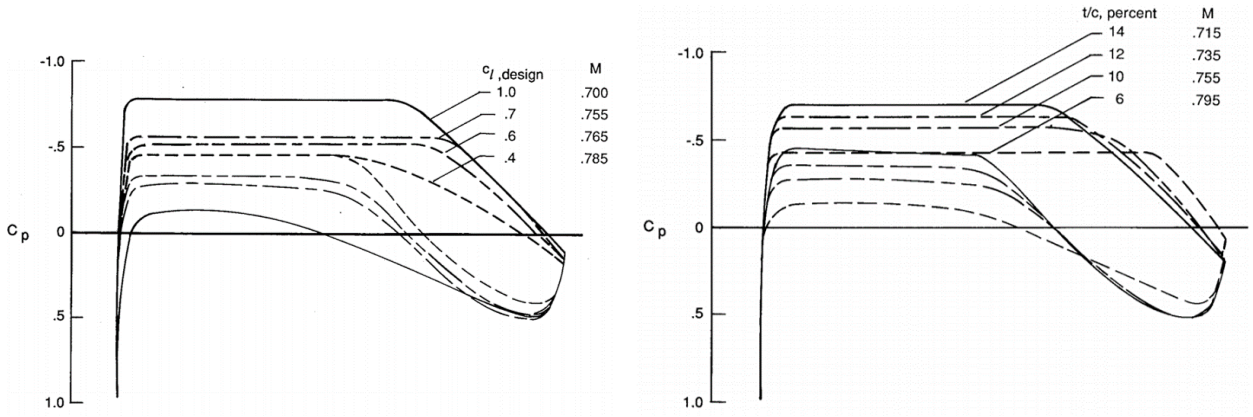


(a) effect of lift coefficient, $\left(\frac{t}{c}\right)_{\text{max}} = 10\%$

(b) effect of thickness, $c_{l_{\text{design}}} = 0.7$

**Fig. 2 NASA supercritical airfoil sonic plateau pressure distributions [11].**

Given the desired $c_{l_{\text{design}}}$ and $M_{\text{DD}}$ for the airfoil, the plateau flight conditions are found from a regression of data in Figs. 27–29 in Ref. [11]:

$$\begin{aligned} M_{\text{plat}} &= \frac{M_{\text{DD}} - 0.0933}{0.906} \\ c_{l_{\text{plat}}} &= c_{l_{\text{design}}} - 0.25 \end{aligned} \tag{4}$$

Figure 3, taken directly from Ref. [11], shows the calculated and experimental values of drag-divergence Mach number for the airfoils in the matrix. The data in the figure can be used to formulate the inverse relationship; that is, given the desired design lift coefficient and drag-divergence Mach number, one can determine the allowable maximum airfoil thickness. The allowable thickness is a value at which it should be possible for an airfoil with the given design lift coefficient to achieve the desired drag-divergence Mach number. Performing a regression on the data yields the following relationship:

$$\text{allowable} \left(\frac{t}{c}\right)_{\text{max}} = \left(0.9753 - 1.1267 M_{\text{DD}}\right)\left(1.0422 + 0.0504 c_{l_{\text{design}}} - 0.1566 c_{l_{\text{design}}}^2\right) \tag{5}$$

This relationship is plotted in Fig. 4, with the circles representing individual airfoils in the matrix.

### C. Parametric Target Pressure Distributions

Once the design lift coefficient and the allowable thickness are determined, a parametric target pressure distribution is specified using eight control points: one each for the stagnation point and trailing edge, and three each for the upper

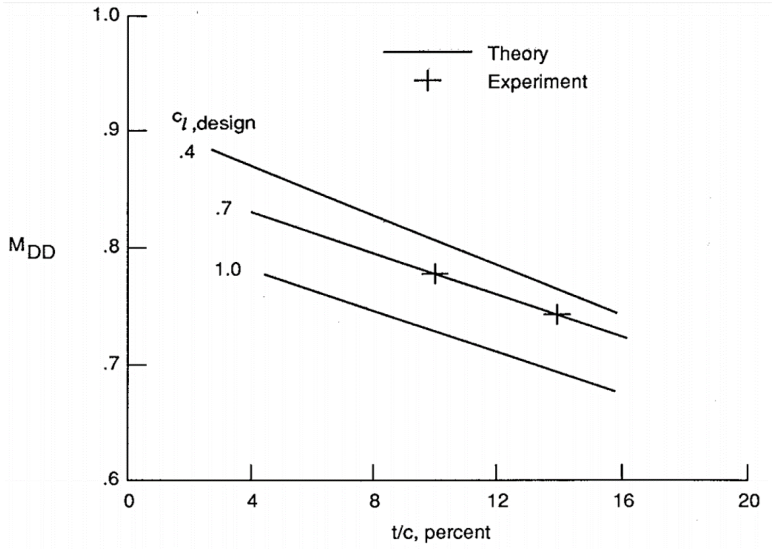


**Fig. 3 Effect of thickness and design lift coefficient on drag-divergence Mach number [11].**

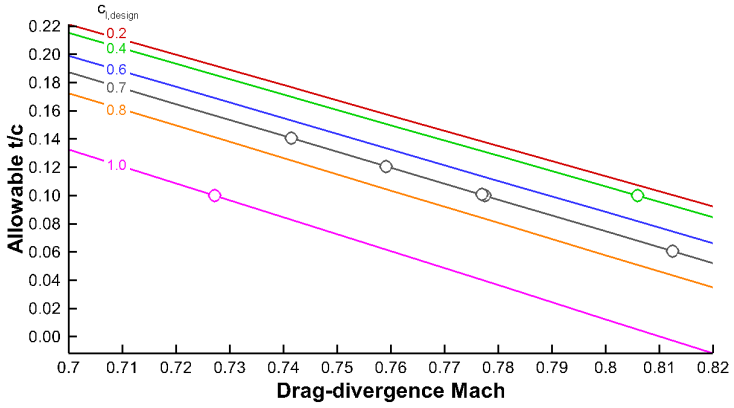


**Fig. 4 Allowable maximum thickness versus desired drag-divergence Mach number and design lift coefficient.**

and lower surfaces (Fig. 5). The pressure distribution between the control points is defined by various polynomials ranging from first- to fourth-order, as indicated in Fig. 5. The polynomials are defined such that both the first and second derivatives are continuous at the control points. The fractional distance at point $p_{2_l}$ is set at 40% to be consistent with the distributions in Fig. 2. The distance at point $p_{2_u}$ is set such that $\mathrm{d}c_p/\mathrm{d}s \leq 2.5$ in the pressure recovery region near the trailing edge, in order to avoid creating an adverse pressure gradient that is too steep and could lead to separation of the flow.

An initial guess at the pressure distribution is created which approximately matches the lift, thickness, and moment coefficient targets for the airfoil. The lift and moment coefficients are approximated as follows:

$$\begin{aligned} c_l &\approx \int_0^1 \left(c_{p_l} - c_{p_u}\right) \mathrm{d}s \\ c_{m_{c/4}} &\approx \int_0^1 \left(c_{p_l} - c_{p_u}\right) \left(s - \frac{1}{4}\right) \mathrm{d}s \end{aligned} \tag{6}$$

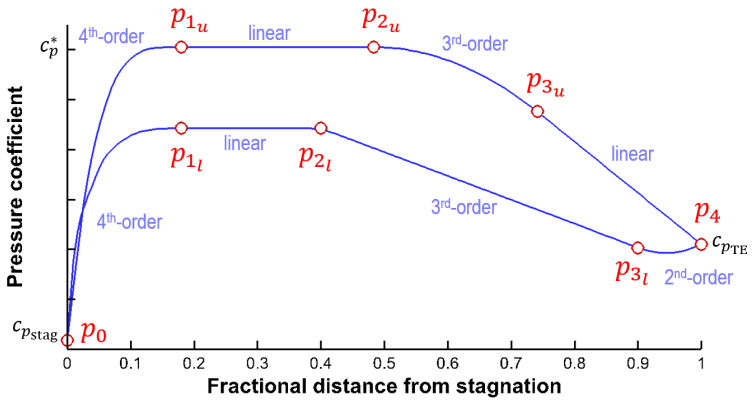


**Fig. 5 Piecewise parametric pressure distribution.**

For the given pressure distribution, the airfoil's maximum thickness is estimated by the following first-order approximation [12]:

$$\left(\frac{t}{c}\right)_{\max} \approx -\frac{\sqrt{1-M_{\text{plat}}^2}}{4}\int_0^1 \left(c_{p_l}+c_{p_u}\right)\mathrm{d}s \tag{7}$$

The shape of the pressure distribution is then iteratively adjusted to simultaneously match the target lift and moment coefficients and desired maximum thickness as follows:

- To increase the lift coefficient, $p_{1_u}$ and $p_{2_u}$ are moved upward while $p_{1_l}$ and $p_{2_l}$ are moved downward. To reduce the lift coefficient, these directions are reversed.
- To increase (or reduce) the magnitude of the moment coefficient, $p_{3_l}$ is moved downward (or upward).
- To increase (or reduce) the thickness, $p_{1_l}$, $p_{2_l}$, $p_{1_u}$, and $p_{2_u}$ are all moved upward (or downward).

This iteration continues until the estimated lift and moment coefficients and maximum thickness are sufficiently close to the target values.

### D. Inverse Design Process

Once the target pressure distribution has been defined, the airfoil shape can be designed using MSES, which is a two-dimensional Euler solver and design code with a tightly coupled integral boundary-layer solution [13]. MSES has a mixed-inverse design mode that simultaneously converges the flow solution with the inverse design problem [14]. In this methodology the design process is currently carried out using an inviscid analysis.

The starting point for the design is a standard NACA 0010 airfoil. Due to the significant differences between the starting pressure distribution and the distribution to be matched, the inverse design process generally cannot be accomplished for the full airfoil at once. Any changes to the lower surface shape to match the prescribed pressure distribution cause a departure from the prescribed upper-surface pressure distribution, and vice versa. In addition, the pressure distribution forward of the suction peak on a given surface typically cannot be matched until the distribution aft of the suction peak is designed to an approximately correct shape. To achieve a complete and robust design process, the design is performed in the following steps:

- Converge the analysis for the original airfoil.
- Mixed inverse design successively on:
    1) lower surface from the suction peak aft
    2) upper surface from the suction peak aft
    3) complete lower surface
    4) complete upper surface
    5) complete lower surface
    6) complete upper surface
    7) . . . etc.
- Steps 5 and 6 are repeated until satisfactory convergence is achieved.

Since the upper and lower surfaces of the airfoil are designed separately, a discontinuity may form across the nose during the process. To remedy this problem, the full airfoil surface is smoothed using a fourth-order B-spline. This step ensures third-order continuity across the nose for acceptable off-design performance and provides a parametric representation of the airfoil surface that can be used to interpolate between the points to any fineness level.

Additional steps may be required to fix deficiencies in the final airfoil design. A residual angle of attack resulting from the design process is fixed by locating the new leading edge and re-normalizing the airfoil for the adjusted chord line. The $c_p$ value at the trailing edge point ($p_4$) might need to be adjusted to correct any difference between the target and actual pressure. Excessively thin or crossed trailing edges are corrected by moving point $p_{3_u}$ upward and/or reducing the magnitude of the target moment coefficient. Finally, too much or too little curvature in the nose region of either the upper or lower surface can be corrected by moving point $p_{u_1}$ or $p_{l_1}$ to the left or right, as illustrated in Fig. 6. Each time one of these control points is moved, the steps in the inverse design process are repeated to adjust the airfoil shape.

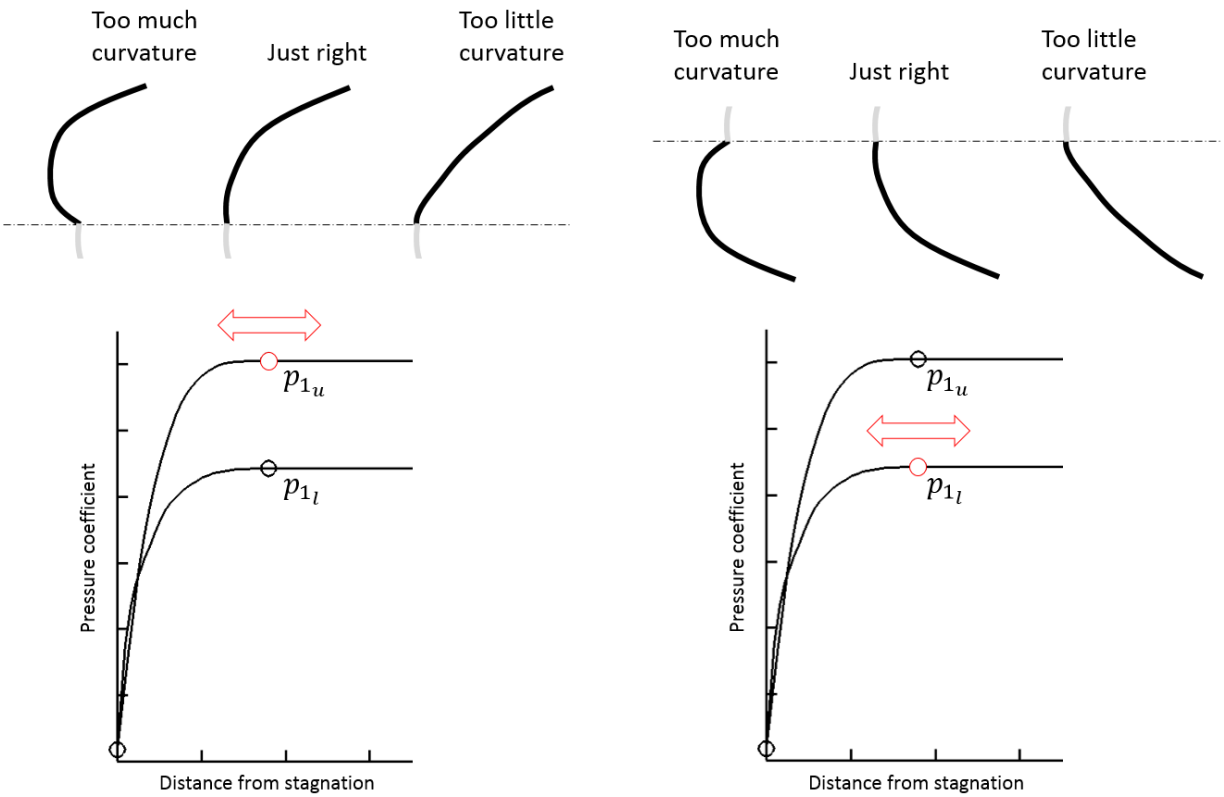


(a) upper surface (b) lower surface

**Fig. 6 Adjusting the pressure distribution to correct nose curvature.**

## III. Example Case

To demonstrate application of the design process, a simplified model of the Boeing 737-200 aircraft is used as an example case. An OpenVSP [15] model of the aircraft is shown in Fig. 7. The flight conditions used for design of the airfoils are given in Table 1. The design process will be demonstrated for the airfoil at 38% of semispan.

For this example, the wing was assumed to be rigid when designing the twist distribution. Figure 8 shows the initial and target spanwise loading distributions for the maximum-range cruise flight condition, and the actual loading after one iteration. Using the modal optimization process, the target loading is effectively matched in the first iteration. Finally, the figure shows the loading distribution at high-speed cruise conditions, which is used to define the design conditions for the individual airfoils.

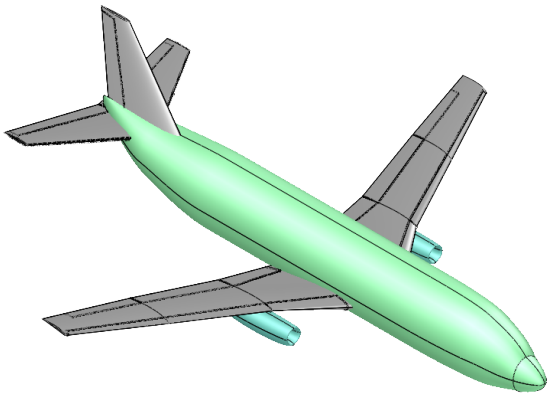

**Fig. 7 Boeing 737-200 OpenVSP model.**

**Table 1 Design Flight Conditions for Example Case.**

| Flight condition | Weight | Mach | Altitude |
|---|---|---|---|
| Maximum-range cruise | 90 000 lb | 0.785 | 32 000 ft |
| High-speed cruise | 112 000 lb | 0.801 | 37 000 ft |
| Drag divergence | 112 000 lb | 0.809 | 37 000 ft |

At 38% of semispan, the wing sweep is 23.4 degrees, so the airfoil was designed for flight conditions of $M_{\text{design}} = 0.735$ and $c_{l_{\text{design}}} = 0.756$, and with a targeted $M_{\text{DD}} = 0.742$. From Eq. (4), this design condition corresponds to sonic-plateau conditions of $M_{\text{plat}} = 0.716$ and $c_{l_{\text{plat}}} = 0.506$. The target moment coefficient was set to $c_{m_{plat}} = -0.14$ based on values for similar design conditions in Ref. [11]. Using Eq. (5), the target value for the maximum thickness was set at 13.2%.

Figure 9 shows the initial, target, and final design pressure distributions for the airfoil. The mixed-inverse process in MSES was able to effectively remove the initial upper-surface shock and produce a shock-free distribution in the final design. The process did not perfectly match the shape of the pressure distribution but was able to produce a sonic-plateau design with the same lift coefficient.

The initial and final airfoil shapes are shown in Fig. 10. The maximum thickness of the final airfoil design is 13.6%, which is very close to the initial target of 13.2%. Figure 11 compares the pressure distributions at the sonic-plateau flight condition and the high-speed cruise design condition. From sonic-plateau conditions, if the lift coefficient and Mach number are increased to the design values, Fig. 11 shows that a shock is created on the upper surface prior to the beginning of the pressure-recovery region. This moderately strong shock can be expected to produce an increase in pressure drag at the design flight condition.

Figure 12 shows the increase in drag during an overspeed maneuver at a constant value of $M\sqrt{c_l}$, corresponding to constant weight and altitude. As expected, the wave drag is nearly zero at the sonic-plateau condition, then increases steadily as the Mach number increases. Using the criterion of Eq. (3), the drag-divergence Mach number was calculated as $M_{\text{DD}} = 0.740$. This is only slightly lower than the target of 0.742 and is higher than the design Mach number of 0.735 as desired.

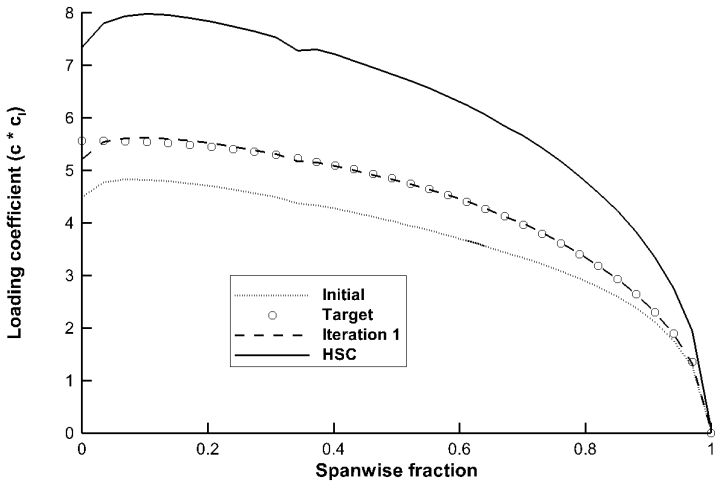


**Fig. 8 Spanwise loading distributions.**

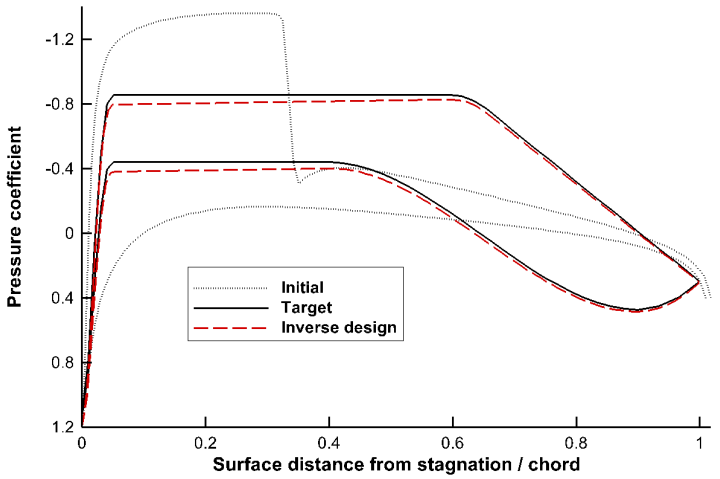


**Fig. 9 Initial, target, and final pressure distributions for airfoil at 38% semispan.**

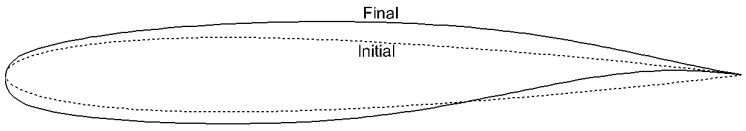


**Fig. 10 Initial and final airfoils.**

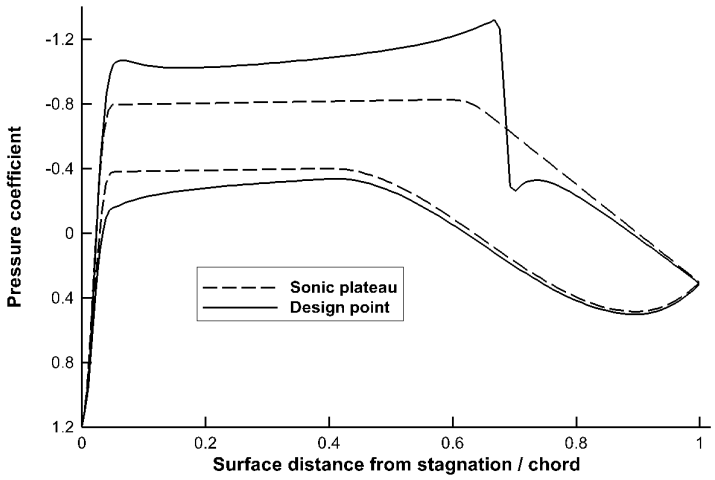


**Fig. 11 Pressure distributions at 38% semispan for sonic plateau and design flight conditions.**

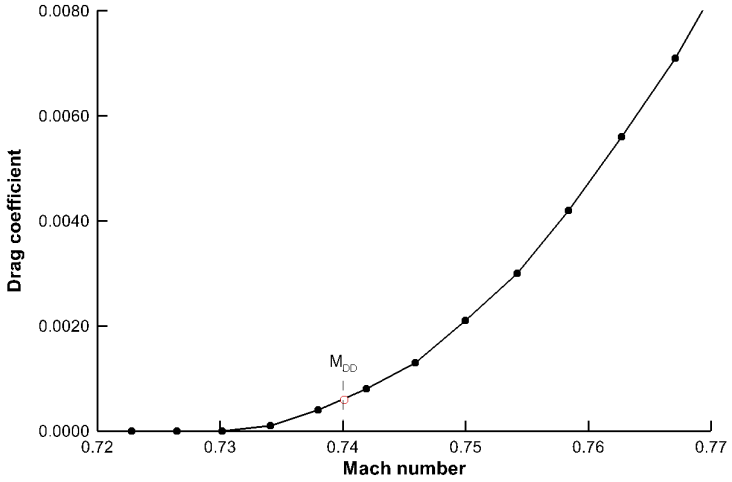


**Fig. 12 Drag coefficient for increasing Mach number, constant $M\sqrt{c_l} = M_{\mathbf{design}}\sqrt{c_{l_{\mathbf{design}}}}$.**

## IV. Concluding Remarks

This paper outlined a means of designing the airfoils of a wing for acceptable drag characteristics at transonic flight conditions. A key aspect of the methodology is the use of a sonic-plateau pressure distribution as the target for an inverse design. The sonic-plateau distribution is easily parameterized and has the advantage of automatically resulting in a smooth airfoil shape without any discontinuities that might be built into the surface due to the presence of a shock in the target pressure distribution. A disadvantage to this approach is the fact that the airfoil is designed at conditions other than the design flight conditions, so control over the performance at design conditions is indirect.

The methodology begins with a modal optimization approach to matching the desired spanwise lift distribution. In the example problem, the process was found to converge to the solution in a single iteration and required approximately 100 seconds on a laptop computer. The methodology then uses an alternating approach to inverse design in MSES, which allows robust convergence of the design problem, even when starting from a geometry which differs greatly from the final design.

The example problem demonstrated that the airfoil design process is quick and robust, with approximately 70 seconds required to design each airfoil. The process still may require manual iteration to fix deficiencies in the leading edge of the designed airfoil (as in Fig. 6), so additional automation in this area will be required to make the approach suitable for use in an automated optimization process.

This methodology could be extended further by including viscosity in the airfoil inverse design process. In order to maintain the robustness of the process, it is likely that this would require a multi-step process; i.e., an inviscid design step to arrive at a design close to the final design, followed by a viscous design step to account for the effects of viscosity.

The methodology used to produce the results in this paper is available as part of Version 1.1.1 of the Higher Order Design Environment, which is available from the NASA Software Catalog at `https://software.nasa.gov/software/LAR-19572-1`.

## Acknowledgments

This work was conducted as part of the NASA Transformational Tools and Technologies Project, led by Dr. Michael Rogers, within the Multi-Disciplinary Design, Analysis and Optimization element, led by Patricia Glaab.

The author wishes to thank Richard Campbell for technical advice and Dr. Wu Li for editorial assistance.

## References

[1] Torenbeek, E., *Synthesis of Subsonic Airplane Design*, Kluwer Academic Publishers, Boston, 1982.

[2] Lane, K. A., Marshall, D. D., and McDonald, R. A., "Lift Superposition and Aerodynamic Twist Optimization for Achieving Desired Lift Distributions," *48th AIAA Aerospace Sciences Meeting Including the New Horizons Forum and Aerospace Exposition*, AIAA 2010–1227, Orlando, FL, 2010. doi:10.2514/6.2010-1227.

[3] Drela, M., *ASWING 5.99 Technical Description—Steady Formulation*, MIT Department of Aeronautics and Astronautics, 2015.

[4] Campbell, R., "Efficient Constrained Design using Navier-Stokes Codes," *13th AIAA Applied Aerodynamics Conference*, AIAA 95–1808, San Diego, CA, 1995. doi:10.2514/6.1995-1808.

[5] Matsushima, K., Takanashi, S., and Iwamiya, T., "Inverse Design Method for Transonic Multiple Wing Systems Using Integral Equations," *Journal of Aircraft*, Vol. 34, No. 3, 1997, pp. 322–329. doi:10.2514/2.2201.

[6] Campbell, R. L., "Efficient Viscous Design of Realistic Aircraft Configurations," AIAA 98–2539, 1998. doi:10.2514/6.1998-2539.

[7] Kim, H.-J., and Rho, O.-H., "Aerodynamic Design of Transonic Wings Using the Target Pressure Optimization Approach," *Journal of Aircraft*, Vol. 35, No. 5, 1998, pp. 671–677. doi:10.2514/2.2374.

[8] II, W. E. M., "Efficient Inverse Aerodynamic Design Method for Subsonic Flows," *Journal of Aircraft*, Vol. 38, No. 5, 2001, pp. 918–923.

[9] Zhang, M., Rizzi, A. W., and Nangia, R. K., "Transonic Airfoils and Wings Design Using Inverse and Direct Methods," *53rd AIAA Aerospace Sciences Meeting*, AIAA 2015–1943, San Diego, CA, 2015. doi:10.2514/6.2015-1943.

[10] Campbell, R. L., and Lynde, M. N., "A Knowledge-Based Optimization Method for Aerodynamic Design," *2019 AIAA Science and Technology Forum and Exposition*, AIAA 2019–1207, San Diego, CA, 2019. doi:10.2514/6.2019-1207.

[11] Harris, C. D., "NASA Supercritical Airfoils – A Matrix of Family-Related Airfoils," NASA TP–2969, 1990.

[12] van Egmond, J. A., "Numerical Optimization of Target Pressure Distributions for Subsonic and Transonic Airfoil Design," *Computational Methods for Aerodynamic Design (Inverse) and Optimization*, AGARD CP 463, Ref. 17, 1990.

[13] Drela, M., and Giles, M. B., "Viscous-Inviscid Analysis of Transonic and Low Reynolds Number Airfoils," *AIAA Journal*, Vol. 25, No. 10, 1986, pp. 1347–1206.

[14] Giles, M. B., and Drela, M., "Two-Dimensional Transonic Aerodynamic Design Method," *AIAA Journal*, Vol. 25, No. 9, 1987, pp. 1199–1355.

[15] Hahn, A., "Vehicle Sketch Pad: A Parametric Geometry Modeler for Conceptual Aircraft Design," *48th AIAA Aerospace Sciences Meeting Including the New Horizons Forum and Aerospace Exposition*, AIAA 2010–657, Orlando, FL, 2010. doi:10.2514/6.2010-657.